Dojo and Hiramatsu *Earth, Planets and Space* (2017) 69:76
DOI 10.1186/s40623-017-0663-x

Earth, Planets and Space

EXPRESS LETTER

Open Access

Spatial variation in coda *Q* in the northeastern part of Niigata–Kobe Tectonic Zone, central Japan: implication of the cause of a high strain rate zone

Masanobu Dojo[1] and Yoshihiro Hiramatsu[2*]

Abstract

We have analyzed the spatial variation in coda *Q* in the northeastern part of a high strain rate zone, the Niigata–Kobe Tectonic Zone (NKTZ), to investigate the cause of the high strain rate by correlating coda *Q* with the differential strain rate and the S-wave velocity. The spatial distributions of coda *Q* in the 2–4 and 4–8 Hz frequency bands are found to be negatively correlated with the differential strain rate. Coda *Q* in the 2–4 Hz frequency band is correlated spatially with the S-wave velocity at a 25 km depth, as has been reported previously. We also find a positive correlation between the perturbation of the S-wave velocity at a 10 km depth and coda *Q* in the 4–8 Hz frequency band, implying that the spatial distribution of coda *Q* in this frequency band is mainly attributed to the heterogeneity of the upper crust. This feature is different from that of the central part of the NKTZ reported previously, which indicates a difference in the cause of the high strain rate. Therefore, we suggest that the high deformation rate in the upper crust, which is characterized by a thick sediment basin, as well as that in the ductile lower crust, contributes to the generation process of the high strain rate on the surface in the northeastern part of the NKTZ.

Keywords: Heterogeneity, Differential strain rate, S-wave velocity, Ductile deformation

Introduction

The occurrence of inland earthquakes is mainly related to active faults, and the recurrence interval of those is generally thousands of years. However, the generation process, such as the stress accumulation on a fault, has not been well resolved compared with the case of interplate earthquakes. The recent development of a nationwide dense network of GPS sensors in Japan has revealed a zone of high strain rate concentration from Niigata to Kobe (Sagiya et al. 2000). This is called the Niigata–Kobe Tectonic Zone (NKTZ) and is about 500 km long and about 100 km wide. There have been many large inland earthquakes along this tectonic zone (Sagiya et al. 2000). The NKTZ, therefore, provides an important focus to help understand the stress accumulation process in a seismogenic zone.

The stress field controls the distribution of microcracks in the crust, thereby modulating the scattering of seismic waves, the seismic wave velocity, and its anisotropy. S-coda waves consist of S-waves scattered by the heterogeneity of the crust (Aki 1969), and the attenuation of S-coda waves, represented as coda *Q*, is considered to be a good indicator of the stress state in the crust (Aki 1980; Hiramatsu et al. 2000). Padhy et al. (2013) analyzed the temporal changes in coda *Q* associated with the 2011 off the Pacific coast of Tohoku earthquake along the Pacific coast of northeastern Japan. They reported that, inside the source region, the value of coda *Q* with center frequencies of 1.25–3.5 Hz decreased by about 10–16% after the earthquake. The pattern of the temporal change matches that in the Tamba region due to the static stress change associated with the 1995 Hyogo-ken Nanbu

*Correspondence: yoshizo@staff.kanazawa-u.ac.jp
[2] School of Natural System, College of Science and Engineering, Kanazawa University, Kakuma, Kanazawa 920-1192, Japan
Full list of author information is available at the end of the article

earthquake in Japan, which is a decrease in coda Q with an increase in stress (Hiramatsu et al. 2000).

Jin and Aki (2005) analyzed the spatial distribution of coda Q over Japan, with the exception of Hokkaido Island. They showed that a low coda Q in low-frequency bands (1–2 and 2–4 Hz) corresponded spatially to the high strain rate zone. Hiramatsu et al. (2013) and Tsuji et al. (2014) conducted detailed analyses of coda Q in the central part of the NKTZ. These studies showed that the spatial distribution of a low coda Q at low frequencies (center frequencies of 1–4 Hz) coincided with low S-wave velocities at a 25 km depth (Matsubara et al. 2008; Nakajima and Hasegawa 2007), while the coda Q at high frequencies (center frequencies of 5 Hz or higher) did not show any characteristic distribution. Carcolé and Sato (2010) conducted the multiple lapse time analysis for the separate estimation of intrinsic and scattering attenuation (Q_i and Q_s), as well as the estimation of coda Q, all over Japan. They showed that the NKTZ is characterized by low coda Q and low Q_i in low-frequency bands (1–2 and 2–4 Hz).

Together with the results of shear wave splitting (Hiramatsu et al. 2010, 2015), Hiramatsu et al. (2013) and Tsuji et al. (2014) suggested that the cause of the high strain rate zone could be attributed to the high deformation rate below the brittle–ductile transition zone in the crust. This idea is in agreement with the weak zone model as a cause of the NKTZ proposed by Iio et al. (2002, 2004), based on the observations of rich water content (Sano and Wakita 1985) and low velocity (Nakajima and Hasegawa 2007) in the lower crust beneath the NKTZ. In his model, plastic flow in the low viscosity area in the lower crust generates a concentration of strain and high seismicity in the upper crust.

In this study, we have investigated the details of the spatial distribution of coda Q in the northeastern part of the NKTZ during the period January 2012–October 2014, and we discuss the origin of the high strain rate.

Data and method

We analyzed 2194 events during the period January 2012–October 2014 in the northeastern part of the NKTZ (Fig. 1). The magnitudes of the events were greater than 1.8 and the focal depths shallower than 30 km. We used seismic waveform data recorded at the stations of the Earthquake Research Institute, University of Tokyo; the Disaster Prevention Research Institute, Kyoto University; the Research Center for Prediction of Earthquakes

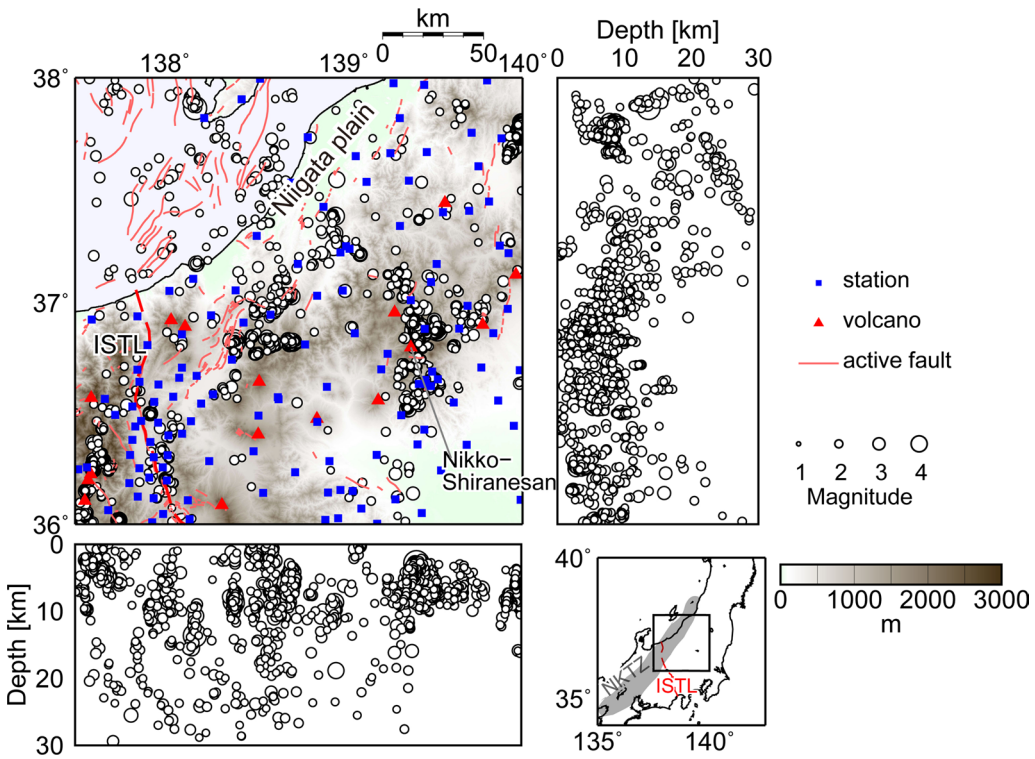

Fig. 1 Spatial distribution of epicenters (*circles*) and stations (*blue squares*) used in this study. *Red lines* show Quaternary active faults (Active Fault Research Group 1991), and *red triangles* show Quaternary active volcanoes. In a lower-right panel, *red lines* show the Itoigawa–Shizuoka Tectonic Line (ISTL) and *a gray zone* shows the Niigata–Kobe Tectonic Zone (NKTZ)

and Volcanic Eruptions, Tohoku University; the Japan Meteorological Agency; and Hi-net data operated by the National Research Institute for Earth Science and Disaster Prevention (Fig. 1). We analyzed these events for which the epicentral distance was within 30 km for each station.

We followed the procedure of Tsuji et al. (2014) to calculate the coda Q, and we applied a band-pass filter to the waveform data in five frequency bands: 1–2, 2–4, 4–8, 8–16, and 16–32 Hz. We calculated the root-mean-square (RMS) amplitude in a moving time window with a duration of $4/f$, where f is the center frequency of each band. Then, we applied the single backscattering model (Aki and Chouet 1975):

$$\ln A_C(f|t) = -\ln t - \pi f Q_C^{-1} t + \text{const}, \quad (1)$$

where $A_C(f|t)$ is the RMS amplitude of the band-pass filtered coda wave at the center frequency f and the lapse time t. For each band, we estimated coda Q by fitting Eq. (1) and averaging over three components at each station using the logarithmic value of Q_C^{-1}. We applied a robust estimation by the criteria of the least absolute deviation in fitting Eq. (1) (Hiramatsu et al. 2000). The time window for the estimation of coda Q was from twice the S-wave travel time to the lapse time of 30 s after the origin time. We excluded the time window of which end is prior to twice the S-wave travel time to avoid the influence of forward scattering. If the coda amplitude reached twice the noise level for each frequency band before the lapse time of 30 s, the end of the time window was set to the time when the amplitude reached twice the noise level. If the time window was <5 s, we did not calculate the coda Q. The window length does not affect significantly the estimation of the coda Q values (Additional file 1: Figures S1 and S2). We also visually confirmed the waveform data and excluded the data having a poor fitting of Eq. (1). The single backscattering model showed that the lapse time 30 s was nearly to the farthest scatters from the station located at 45 km (Jin and Aki 2005). An example of the analysis is shown in Fig. 2.

Finally, we use the stations at which we obtained the values of coda Q for more than five events to map the spatial distribution of coda Q. We calculated the average of the logarithmic value of Q_C^{-1} at each station for each band. We smoothed the average value spatially over an area of 10 min longitude × 10 min latitude in 1 min squares by using the surface command of the Generic Mapping Tools (GMT) software (Wessel and Smith 1998) and constructed the map of the spatial distribution of coda Q in the study area.

Results

Figure 3 shows the spatial distribution of coda Q during 2012–2014. We recognize broadly three different patterns of the distribution depending on the frequency bands: low frequencies (1–2 and 2–4 Hz), middle frequencies (4–8 and 8–16 Hz), and a high frequency (16–32 Hz). A typical value of the standard deviation of the average of the logarithmic coda Q^{-1} is 0.1, with the exception of some stations in 1–2 Hz frequency band (Additional file 1: Figure S3).

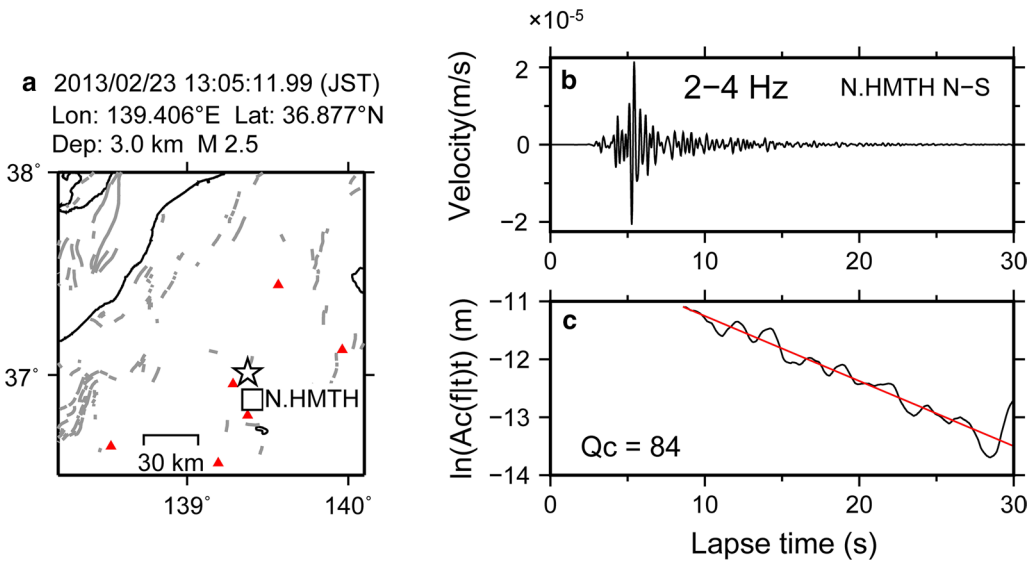

Fig. 2 An example of the estimation of coda Q. **a** Locations of an epicenter (*star*) and a station (*square*). **b** Seismic velocity waveforms at the station N.HMTH. **c** Fitting of Eq. (1) (*red line*) to RMS amplitudes (*black line*)

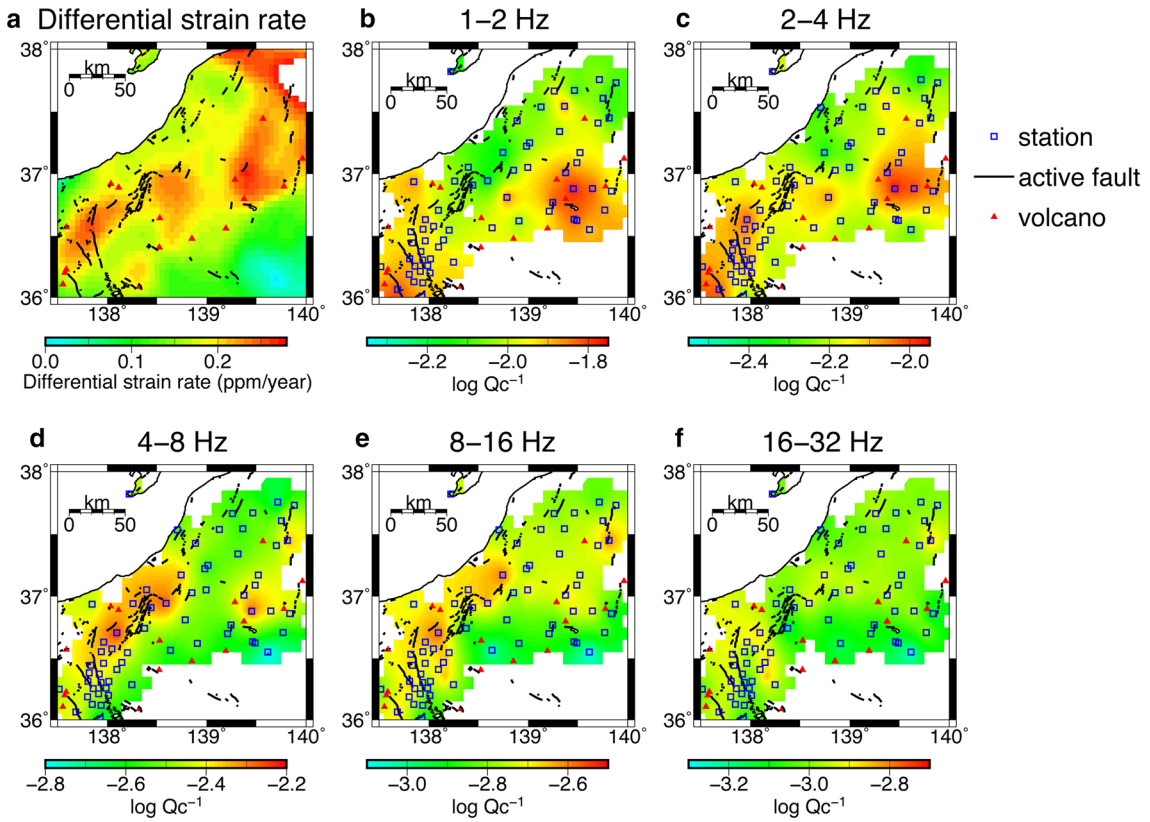

Fig. 3 Spatial distributions of **a** the differential strain rate during 2012–2014, and **b**–**e** the coda *Q* at five frequency bands in this study area. *Blue squares* are stations used to draw the coda *Q* maps, in five frequency bands in this study area, *black lines* show Quaternary active faults, and *red triangles* show Quaternary active volcanoes

In the low-frequency bands, we recognize that low coda *Q* is distributed around the Itoigawa–Shizuoka Tectonic Line (ISTL), while high coda *Q* is distributed around the Niigata plain. This distribution is similar to that of coda *Q* at 1–2 Hz reported by Carcolé and Sato (2010) although the condition of their analysis is different from ours. We also find low coda *Q* around some active volcanoes, especially to the southeast of Nikko-Shiranesan, while not so low coda *Q* around other ones, implying that active volcanoes are not common sources of low coda *Q* in low-frequency bands. On the other hand, high coda *Q* in the low-frequency bands along the faults around the Niigata plain is found in this study area, although Hiramatsu et al. (2013) showed a low coda *Q* zone at low frequencies (center frequency of 4.0 Hz or less) along the Atotsugawa fault zone.

In the middle-frequency bands, a low coda *Q* zone is distributed from the southwestern Niigata plain to the ISTL, while a high coda *Q* zone is found in the other part of this study area. This spatial pattern is coincident with that of Carcolé and Sato (2010). Jin and Aki (2005) showed that low coda *Q* zones in the middle-frequency bands were found around active volcanic areas in the Kyushu and Tohoku districts. A low coda *Q* zone in the middle-frequency bands is recognized around volcanoes near the ISTL, while a high coda *Q* zone is found around volcanoes in the north Kanto district. These spatial distributions, observed in the low- and middle-frequency bands, are somewhat different from those of Jin and Aki (2005). The differences may be the result of a lower resolution of the spatial distribution of the coda *Q* of Jin and Aki (2005) than that in this study because they only used seismic records at Hi-net stations.

In the high-frequency band, it is difficult to find a distinct pattern of the spatial distribution of coda *Q* that is related closely to the fault zones, or the high strain rate zone.

We compare the spatial distribution of coda *Q* versus the differential strain rate in Fig. 4a–e. The differential strain rate is calculated by subtracting the value of the principal strain rate of the compression axis from that of the extension axis, which is twice that of the shear strain rate. In this study, we use the strain rate estimated from GNSS data during January 2012–October 2014

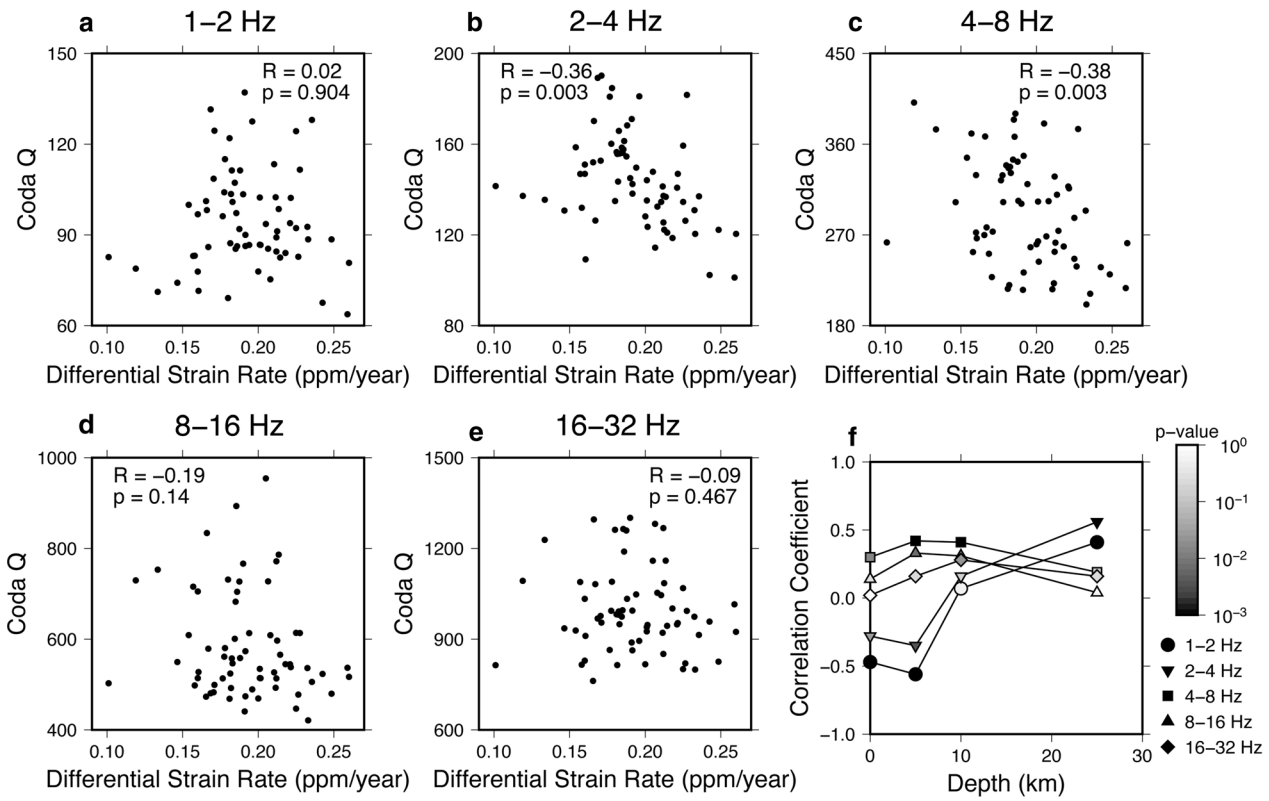

Fig. 4 **a**–**e** Plot of differential strain rate versus coda *Q* at five frequency bands, and **f** plot of depth versus the correlation coefficient between the coda *Q* and the S-wave velocity (Nakajima and Hasegawa 2007) in this study area. *The gray scale* shows the *p* value

(Nishimura 2015, personal communication). We plot the differential strain rate versus the coda *Q* at five frequency bands at every 0.2° of the latitude and longitude (Fig. 4a–e). A weak negative correlation is found between the coda *Q*, in the 2–4 and 4–8 Hz frequency bands, and the differential strain rate, while no correlation is evident for the other frequency bands. A small p value of 0.003 confirms that the correlation in the 2–4 and 4–8 Hz frequency bands is statistically significant.

We also compare the spatial distributions of coda *Q* and the S-wave velocity at 0, 5, 10, and 25 km depths estimated by seismic tomography (Nakajima and Hasegawa 2007). We focus here on the distribution of the S-wave velocity because coda waves consist mainly of S-waves. Figure 4f shows a plot of the correlation coefficients, between the spatial distribution of coda *Q* in each frequency band and the S-wave velocity, with depth. The correlation coefficient between coda *Q* and the S-wave velocity at a 10 km depth is statistically significant in the frequency ranges 4–8 Hz (0.41, $p = 0.001$) and 8–16 Hz (0.31, $p = 0.011$). The correlation coefficient between coda *Q* and the S-wave velocity at a 25 km depth is statistically significant in the ranges 1–2 Hz (0.41, $p = 0.001$) and 2–4 Hz (0.56, $p < 0.001$). Here we note weak positive correlations with a statistical significance between coda *Q* in the middle-frequency bands and the S-wave velocity at a 10 km depth, and between coda *Q* in the low-frequency bands and the S-wave velocity at a 25 km depth.

Discussion

We recognize two distinct features of the spatial distribution of coda *Q*: (1) the weak negative correlations between the spatial distribution of coda *Q* in the 2–4 and 4–8 Hz frequency bands and that of the differential strain rate, and (2) the weak positive correlations between the spatial distribution of coda *Q* in the middle-frequency bands and the S-wave velocity at a 10 km depth, and between coda *Q* in the low-frequency bands and the S-wave velocity at a 25 km depth. We discuss here a cause of the high strain rate in the northeastern part of the NKTZ from these features and comparisons of the results of previous works on coda *Q* in the NKTZ.

Previous works have shown that the high strain rate zone is characterized by a low coda *Q* in the lower-frequency bands in the NKTZ (Jin and Aki 2005; Hiramatsu et al. 2013; Tsuji et al. 2014) and have suggested that, in the central part of the NKTZ, the cause of the high strain rate zone could be attributed to the high deformation

rate below the brittle–ductile transition zone in the crust where the lower crust is characterized by low velocity of S-wave (Hiramatsu et al. 2010, 2013; Tsuji et al. 2014). However, in this study area, we identify a weak negative correlation, not only in a low-frequency band (2–4 Hz) but also in a middle-frequency band (4–8 Hz). This suggests that the generation process of the high strain rate zone in the northeastern part of the NKTZ differs from that in the central part of the NKTZ, i.e., along the Atotsugawa fault zone (Hiramatsu et al. 2013) and around the source area of the 1891 Nobi earthquake (Tsuji et al. 2014). To examine the difference, we have to distinguish a sensitive zone of coda Q in the low- and middle-frequency bands in the crust through a spatial correlation between coda Q and the S-wave velocity.

A weak positive correlation between the spatial distribution of coda Q in the 2–4 Hz frequency band and that of the S-wave velocity at a 25 km depth in this study is interpreted to indicate that the spatial distribution of coda Q in the 2–4 Hz frequency band reflects the heterogeneity in the lower crust. This result is in agreement with that of Hiramatsu et al. (2013) and Tsuji et al. (2014), which reported the correspondence of the spatial distribution of coda Q with the S-wave velocity at a 25 km depth and suggested that the high deformation rate in the lower crust is a cause of the high strain rate. On the other hand, in this study area, we recognize a positive correlation between the coda Q in the middle frequencies and the S-wave velocity at a 10 km depth. It is likely to interpret that the coda Q in the middle frequencies reflects the heterogeneity in the upper crust.

Nakajima and Hasegawa (2007) showed that the S-wave velocity structures differed in the east and in the west of the ISTL as a boundary. A distinct low-velocity zone of the S-wave velocity is distributed in the upper crust on the eastern side of the ISTL, which corresponds to the northeastern part of the NKTZ, while this is the case in the lower crust on the western side of the ISTL, which corresponds to the central part of the NKTZ. They pointed out that the low-velocity zone in the upper crust in the northeastern part of the NKTZ is attributed to the Niigata sedimentary basin. This large difference in the S-wave velocity structures implies a difference in the generation process of the high strain rate between the northeastern and the central parts of the NKTZ.

The observed facts in the 4–8 Hz frequency band, viz. the negative correlation between the coda Q and the differential strain rate, and the positive correlation between the coda Q and the S-wave velocity at a 10 km depth, suggest that the deformation in the upper crust plays another important role in the generation of the high strain rate on the surface in the northeastern NKTZ. The upper crust in the northeastern NKTZ is characterized by a thick sedimentary basin, which may reduce the strength of the upper crust. If this is the case, the deformation in the upper crust is likely to contribute proactively to the generation of the high strain rate zone as suggested by Nakajima and Hasegawa (2007). Structure-induced anisotropy observed dominantly in the northeastern NKTZ (Hiramatsu et al. 2010) might support this possibility. Alternatively, a small correlation coefficient between coda Q and the strain rate at the 2–4 Hz frequency band is possibly interpreted to mean that the deformation rate in the lower crust in the northeastern part might be smaller than that in the central part. The lower crust in this study area, characterized by a higher velocity than the central part of the NKTZ, is consistent with this idea, because high S-wave velocity requires high rigidity, which might act as an obstruction to deform. Therefore, the correlations in the middle-frequency range seem more conspicuous in the northeastern part than in the central part of the NKTZ.

Recently, Nakajima and Matsuzawa (2017) obtained three-dimensional P-wave attenuation structure beneath the NKTZ and pointed out that the high-attenuation areas corresponded to the low-velocity areas and vice versa. They revealed, together with three-dimensional P-wave velocity structure, that the lower crust west of the ISTL and the upper crust east of the ISTL are characterized by high attenuation and low velocity. From these facts, Nakajima and Matsuzawa (2017) concluded that the differences in the depths of elastically weakened parts of crust probably result in a first-order spatial variation in surface deformation, which is in agreement with our discussion through the correlation between the coda Q, the strain rate, and the S-wave velocity.

In this study, we also observe a negative correlation between the spatial distribution of coda Q in the lower-frequency bands and the S-wave velocity in the upper crust (Fig. 4f). We consider that this correlation does not relate to the generation of the high strain rate zone, because the sign of the correlation is opposite to that reported in previous studies (Jin and Aki 2005; Hiramatsu et al. 2013; Tsuji et al. 2014). The negative correlation observed here is mainly attributed to a relatively high coda Q in the low-frequency bands in the Niigata plain. Seismograms at stations on a soft sediment layer tend to record longer oscillations, leading to a higher coda Q estimation than at stations on hard rock. Thus, this correlation may reflect geological features in this study area, although future work is required to resolve this.

The observed frequency dependency of coda Q is interpreted by a characteristic scale length of the crustal heterogeneity (Hiramatsu et al. 2013; Tsuji et al. 2014). A numerical simulation shows that the most effective scattering occurs in the case that the wavelength is twice

the characteristic scale of the scatterer (Yomogida and Benites 1995). Applying this relation, together with the average S-wave velocity at a 10 km depth and at a 25 km depth (Nakajima and Hasegawa 2007), we can estimate a characteristic scale length is to be 0.4–0.9 km at a 10 km depth and 1–2 km at a 25 km depth.

Finally, there is one aspect which should be noted. The analysis period of this study is January 2012–October 2014, i.e., after the 2011 off the Pacific coast of Tohoku earthquake, and several researchers have reported a temporal change in the scattering environment in the crust in northeast Japan after the earthquake (e.g., Takagi and Okada 2012; Kato et al. 2013; Padhy et al. 2013). These studies reported that there are significant variations in the S-wave velocity, or the scattering environment in/around the source area, but no systematic and/or significant variations in the other areas where this study area is included. Therefore, we infer that the temporal variation in coda Q caused by the 2011 earthquake is not significant in this study area, as is also the case in the source area of the 1891 Nobi earthquake (Tsuji et al. 2014), although it is difficult to completely exclude the possibility of the temporal variation. This possibility, and the detailed spatial variation in coda Q prior to the 2011 earthquake in this study area, will be examined in future work.

Conclusions

We have determined the spatial distribution of coda Q in the northeastern part of the NKTZ in order to investigate a cause of high strain rate from the analyses of waveform data in this area. In the low-frequency bands, low coda Q is distributed around the ISTL and some volcanoes, while high coda Q is distributed around the Niigata plain. In the middle-frequency bands, a low coda Q zone is distributed from the southwestern Niigata plain to the ISTL, while a high coda Q zone is found in the other part, around volcanoes in the north Kanto district. In the high-frequency band, we do not find a distinct pattern of the spatial distribution of coda Q that is related closely to the fault zones, or the high strain rate zone. We found that a weak negative correlation exists between the coda Q and the differential strain rate in the 2–4 and 4–8 Hz frequency bands. Positive correlations are found between the perturbations of the S-wave velocity at a 25 km depth and coda Q in the low-frequency bands, and between the perturbations of the S-wave velocity at a 10 km depth and the coda Q in the middle-frequency bands. In the northeastern part of the NKTZ, these facts imply that the spatial distributions of coda Q in the low- and middle-frequency bands reflect mainly the heterogeneity of the lower crust and the upper crust, respectively. These relations are different from those of previous studies in the central part of the NKTZ. Therefore, we consider that a different cause of the high strain rate zone is likely to exist between the central and the northeastern parts of the NKTZ. We suggest that the deformation in the upper crust, as well as the ductile deformation in the lower crust, may be a dominant cause of the high strain rate in the northeastern part of the NKTZ.

Additional file

Additional file 1. Figure S1. The histogram of the time window length in each frequency band. **Figure S2.** The plot of the time window length versus the value of the coda Q in each frequency band. **Figure S3.** The spatial distribution of the standard deviation of the average value of the coda Q in each frequency band.

Abbreviations

NKTZ: Niigata–Kobe Tectonic Zone; ISTL: Itoigawa–Shizuoka Tectonic Line; GMT: Generic Mapping Tools.

Authors' contributions

MD and YH conducted the analyses and drafted the manuscript. All authors read and approved the final manuscript.

Author details

[1] Graduate School of Natural Science and Technology, Kanazawa University, Kakuma, Kanazawa 920-1192, Japan. [2] School of Natural System, College of Science and Engineering, Kanazawa University, Kakuma, Kanazawa 920-1192, Japan.

Acknowledgements

We thank the National Research Institute for Earth Science and Disaster Prevention, the Japan Meteorological Agency, Tokyo University, Kyoto University, and Tohoku University, for allowing us to use waveform data collected at each online station. We are grateful to Junichi Nakajima and Takuya Nishimura for providing us with seismic tomography data and with strain rate data, respectively. The constructive comments of anonymous reviewers are helpful to improve the manuscript. All figures were made using GMT software (Wessel and Smith 1998). This study is supported by JSPS KAKENHI Grant Number 261090003.

Competing interests

The authors declare that they have no competing interests.

Publisher's Note

Received: 26 January 2017 Accepted: 29 May 2017
Published online: 05 June 2017

References

Active Fault Research Group (1991) In active faults in Japan: sheet map and inventories (Revised edn.). University of Tokyo Press, Tokyo **(in Japanese)**

Aki K (1969) Analysis of the seismic coda of local earthquakes as scattered waves. J Geophys Res 74:615–631

Aki K (1980) Scattering and attenuation of shear waves in the lithosphere. J Geophys Res 85:6496–6504

Aki K, Chouet B (1975) Origin of coda waves: source, attenuation and scattering effects. J Geophys Res 80:3322–3342

Carcolé E, Sato H (2010) Spatial distribution of scattering loss and intrinsic absorption of short-period *S* waves in the lithosphere of Japan on the basis of the multiple lapse time window analysis of Hi-net data. Geophys J Int 180:268–290

Hiramatsu Y, Hayashi N, Furumoto M, Katao H (2000) Temporal changes in coda Q^{-1} and *b*-value due to the static stress change associated with the 1995 Hyogo-ken Nanbu earthquake. J Geophys Res 105:6141–6151

Hiramatsu Y, Iwatsuki K, Ueyama S, Iidaka T, The Japanese University Group of the Joint Seismic Observations at NKTZ (2010) Spatial variation in shear wave splitting of the upper crust in the zone of inland high strain rate, central Japan. Earth Planets Space 62:675–684. doi:10.5047/eps.2010.08.003

Hiramatsu Y, Sawada A, Yamauchi Y, Ueyama S, Nishigami K, Kurashimo E, the Japanese University Group of the Joint Seismic Observations at NKTZ (2013) Spatial variation in coda *Q* and stressing rate around the Atotsugawa fault zone in a high strain rate zone, central Japan. Earth Planets Space 65:115–119. doi:10.5047/eps.2012.08.012

Hiramatsu Y, Iidaka T, the Research Group for the Joint Seismic Observations at the Nobi Area (2015) Stress state in the upper crust around the source region of the 1891 Nobi earthquake through shear wave polarization anisotropy. Earth Planets Space 67:52. doi:10.1186/s40623-015-0220-4

Iio Y, Sagiya T, Kobayashi Y, Shiozaki I (2002) Water weakened lower crust and its role in the concentrated deformation in the Japanese Islands. Earth Planet Sci Lett 203:245–253

Iio Y, Sagiya T, Kobayashi Y (2004) Origin of the concentrated deformation zone in the Japanese Islands and stress accumulation process of intraplate earthquakes. Earth Planets Space 56:831–842. doi:10.1186/BF03353090

Jin A, Aki K (2005) High-resolution maps of Coda Q in Japan and their interpretation by the brittle–ductile interaction hypothesis. Earth Planets Space 57:403–409. doi:10.1186/BF03351825

Kato A, Fukuda J, Obara K (2013) Response of seismicity to static and dynamic stress changes induced by the 2011 M9.0 Tohoku-Oki earthquake. Geophys Res Lett. doi:10.1002/grl.50699

Matsubara M, Obara K, Kasahara K (2008) Three-dimensional P- and S-wave velocity structures beneath the Japan Islands obtained by high-density seismic stations by seismic tomography. Tectonophysics 454:86–103

Nakajima J, Hasegawa A (2007) Deep crustal structure along the Niigata–Kobe Tectonic Zone, Japan: its origin and segmentation. Earth Planets Space 59:e5–e8. doi:10.1186/BF03352677

Nakajima J, Matsuzawa T (2017) Anelastic properties beneath the Niigata–Kobe Tectonic Zone, Japan. Earth Planets Space 69:33. doi:10.1186/s40623-017-0619-1

Padhy S, Takemura S, Takemoto T, Maeda T, Furumura T (2013) Spatial and temporal variation in coda attenuation associated with the 2011 off the Pacific coast of Tohoku, Japan (Mw 9) earthquake. Bull Seismol Soc Am 103:1411–1428

Sagiya T, Miyazaki S, Tada T (2000) Continuous GPS array and present-day crustal deformation of Japan. PAGEOPH 157:2003–2322

Sano O, Wakita H (1985) Geographical distribution of 3He/4He ratios in Japan: implications for arc tectonics and incipient magmatism. J Geophys Res 88:8729–8741

Takagi R, Okada T (2012) Temporal change in shear velocity and polarization anisotropy related to the 2011 M9.0 Tohoku-Oki earthquake examined using KiK-net vertical array data. Geophys Res Lett 39:L09310. doi:10.1029/2012GL051342

Tsuji S, Hiramatsu Y, the Japanese University Group of the Joint Seismic Observations at the Area of Nobi Earthquake (2014) Spatial variation in coda *Q* around the Nobi fault zone, central Japan: relation to S-wave velocity and seismicity. Earth Planets Space 66:97. doi:10.1186/1880-5981-66-97

Wessel P, Smith WHF (1998) New, improved version of generic mapping tools released. EOS Trans Am Geophys Union 79:579

Yomogida K, Benites R (1995) Relation between direct wave *Q* and coda *Q*: a numerical approach. Geophys J Int 123:471–483